

# Synthesis and characterization of curcumin-encapsulated loaded on carboxymethyl cellulose with docking validation as $\alpha$ -amylase and $\alpha$ -glucosidase inhibitors

Abdulrahman A. Almehezia<sup>1</sup>, Mohamed A. Al-Omar<sup>1</sup>, Abdulrahman M. Al-Obaid<sup>1</sup>, Ahmed M. Naglah<sup>1</sup>, Mashooq A. Bhat<sup>1</sup>, Hazem A. Ghabbour<sup>2, 3</sup>, Tamer K. Khatab<sup>4</sup>, Ashraf S. Hassan<sup>4\*</sup>

<sup>1</sup>Department of Pharmaceutical Chemistry, College of Pharmacy, King Saud University, P.O. Box 2457, Riyadh 11451, Saudi Arabia

<sup>2</sup>School of health and biomedical sciences, RMIT University, Melbourne 3083, Australia

<sup>3</sup>Department of Medicinal Chemistry, Faculty of Pharmacy, University of Mansoura, Mansoura 35516, Egypt

<sup>4</sup>Organometallic and Organometalloid Chemistry Department, National Research Centre, Dokki 12622, Cairo, Egypt

\*Corresponding author: e-mail: ashraf\_salmoon@yahoo.com

In reaction to the expanding predominance of diabetes mellitus, curcumin nanoparticles stacked on carboxymethyl cellulose (CMC) composite were effectively synthesized, characterized, and examined utilizing UV/Vis and FTIR spectroscopy combined with transmission electron microscopy (TEM). The bioactivity of curcumin (Cur), carboxymethyl cellulose (CMC), and curcumin nanoparticles stacked with carboxymethyl cellulose (CUR-CMC) was tried through atomic docking approval as an  $\alpha$ -amylase and  $\alpha$ -glucosidase inhibitor. The conclusion illustrated that the curcumin-supported CMC is more potent than CUR itself the validation presented is compared with acarbose as a reference molecule and then CUR-CMC can presented as promising in curing hyperglycemia by decreasing the absorption of glucose.

**Keywords:** Curcumin, Carboxymethyl cellulose,  $\alpha$ -Amylase,  $\alpha$ -Glucosidase, Diabetes mellitus treatment.

## INTRODUCTION

Diabetes mellitus (DM) is a medical case marked by high blood glucose levels (hyperglycemia) caused by defective insulin production. The data from the International Diabetes Federation (IDF) indicates that diabetes patients in 2019 were counted approximately 463 million. However, diabetes patients in 2024 will be increased to approximately 700 million<sup>1</sup>. There are two types of diabetes patients: type I (insulin-dependent) type II (non-insulin dependent)<sup>2</sup>. Type II diabetes is the most common type of diabetes, accounting for almost 90%. Diabetes II is a metabolic disease that causes insulin resistance and pancreas  $\beta$ -cell dysfunctions as a result of uncontrolled high blood sugar levels<sup>3</sup>.

There are various drugs available to treat this metabolic disease, classified into three main categories: 1) insulin secretagogues (sulfonylureas), 2) insulin sensitizers (biguanides), and 3)  $\alpha$ -glucosidase inhibitors (acarbose)<sup>4</sup>. In the first two types of long-term therapy, many side effects have appeared, such as hypoglycemia, renal dysfunction, and hepatic diseases<sup>5</sup>. Hence, the third class became safer in focused on decreasing glucose absorption in the intestine through the inhibition of enzymes like  $\alpha$ -glucosidase and  $\alpha$ -amylase that are responsible for the saccharides' hydrolysis to glucose<sup>6</sup>. Acarbose (**I**, **Figure 1**) is presented as an oligosaccharide that acts as an inhibitor of  $\alpha$ -amylase and  $\alpha$ -glucosidase enzymes<sup>7</sup>.

Curcumin (**II**, **Figure 1**) is located in turmeric. The benefits and advantages of curcumin include being a highly potent, non-toxic, and bioactive agent. However, its low aqueous solubility and poor bioavailability of curcumin are their disfavours<sup>8</sup>. Nanoparticles of curcumin (nano-curcumin) improve its aqueous-phase solubility<sup>9</sup>. Recently, curcumin derivatives possess pharmacological applications such as antioxidant, anti-inflammatory<sup>10</sup>, anticancer<sup>11</sup>. Furthermore, they have been established

to have anti-Alzheimer properties in various *in vivo* and *in vitro* studies<sup>12</sup>.

Carboxymethyl cellulose (CMC, **III**, **Figure 1**) possesses distinct properties such as being anionic and water-soluble; therefore, it is a promising cellulose derivative<sup>13</sup>. Carboxymethyl cellulose (CMC) is used in various important applications such as smart biinks for 3D bioprinting<sup>14</sup>, biodegradable polymer for packaging material<sup>15</sup>, and as drug carriers in clinical fields<sup>16</sup>.

Drug discovery and design are major challenges, especially in the current world with various health problems<sup>17</sup>. Molecular docking, a structure-based computational method, has played a crucial role in making drug discovery faster, cheaper, and more effective. It generates the binding energy and affinity between ligands and targets, making it a significant tool for predicting drug-protein interactions<sup>18, 19</sup>.

From the above facts about diabetes mellitus (DM), curcumin (CUR, **I**), and carboxymethyl cellulose (CMC, **III**), molecular docking, with our research goals<sup>20–26</sup>. Therefore, the present study aims to synthesize curcumin nanoparticles loaded with carboxymethyl cellulose and explore its bioactivity for potential use in the treatment of diabetes mellitus against  $\alpha$ -amylase and  $\alpha$ -glucosidase enzyme inhibition through a molecular docking study.

## EXPERIMENTAL

### Materials

Curcumin (CUR, **I**) was obtained from Indus Company (India). Carboxymethyl cellulose (CMC, **III**) was purchased from Sigma-Aldrich Company.

### Synthesis of curcumin nanoparticles (nano-curcumin)

Curcumin nanoparticles were prepared using the hydrothermal squeeze method<sup>27</sup>. Specifically, 15 grams of commercial CUR powder “XPRS Nutra organic turmeric

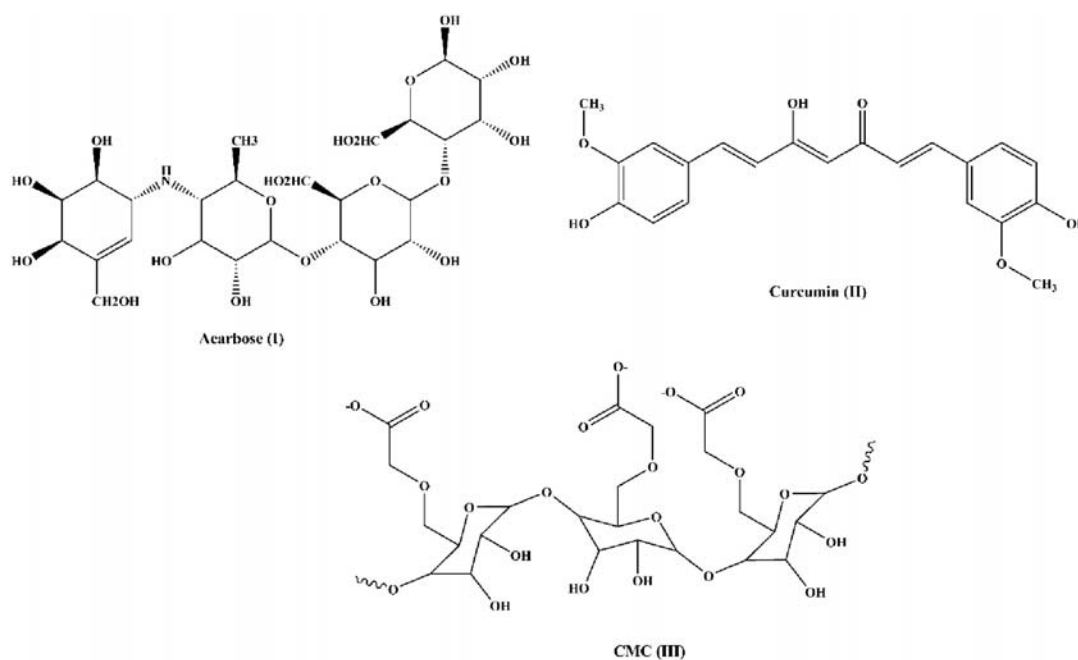


**Figure 1.** The structure of acarbose (I), curcumin (II), and carboxymethyl cellulose (CMC, III)

curcumin powder extract 10:1 - premium USDA<sup>®</sup> (containing > 95% curcuminoids) was dissolved in 70 mL of double distilled water with the addition of two drops of dimethyl sulfoxide (DMSO). After stirring for 5 minutes in a 100 mL beaker, the solution was transferred to a 100 mL Teflon-lined stainless-steel autoclave. The autoclave was placed in an electric oven at 100–150 °C for 12 hours without stirring. The resulting solution was subjected to vacuum distillation to remove 50% of the solvent, and the product was separated by centrifugation at 8000 rpm for 10 minutes. The precipitate was then cooled to room temperature, washed with distilled water, and dried at 60–70 °C for 3 hours.

#### Synthesis of curcumin-loaded polymer nano-composite

The CMC is easily soluble in water due to its highly hygroscopic nature. The solubility of CMC in water is measured by the degree of substitution, which refers to the number of hydroxyl groups substituted by sodium carboxymethyl. Curcumin-loaded polymer nanocomposite thin films were prepared using a traditional solution casting method:

(1) Pre-calculated amounts of carboxymethyl cellulose (CMC) solutions (5 wt %) were prepared by directly dissolving CMC in deionized water under constant stirring, and curcumin nanoparticles were mixed in an aqueous solution until a completely clear, homogeneous, yellowish-colored solution was obtained.

(2) The solution was then poured into a plastic Petri dish and kept in an incubator adjusted at 50°C for about 24 hours. Thin films were then peeled from the dishes and kept in a drying place until use.

#### Nanoparticles characterization

An ultraviolet-visible spectrophotometer (NIR - JASCO Japan, V-570 UV/VIS; range 200–1100 nm) was used to obtain the maximum wavelength of the prepared particles. Fourier transform infrared (FTIR) type Mattson 5000 FT-IR spectrophotometer (range 4000–400 cm<sup>-1</sup>) was used to get the prepared particles FT-IR spectra. The prepared particles underwent grinding with 0.1 g anhy-

drous KBr in a ceramic mortar and were subjected to a pressure of 4 tons per cm<sup>2</sup> until clear transparent discs were obtained. All samples were measured immediately to avoid any moisture. Transmission electron microscopy (TEM) of the JEOL-JEM-2100 instrument, Japan, was used to investigate the prepared particle size.

#### Molecular docking protocol

The MOE 2015.10 software was utilized to conduct the docking protocol according to established standards<sup>28–30</sup>. The  $\alpha$ -amylase and  $\alpha$ -glucosidase proteins were obtained from the Protein Data Bank (PDB) through the mdb file (PDB code: 1BAG and 7D9C) and subjected to this protocol.

## RESULTS AND DISCUSSION

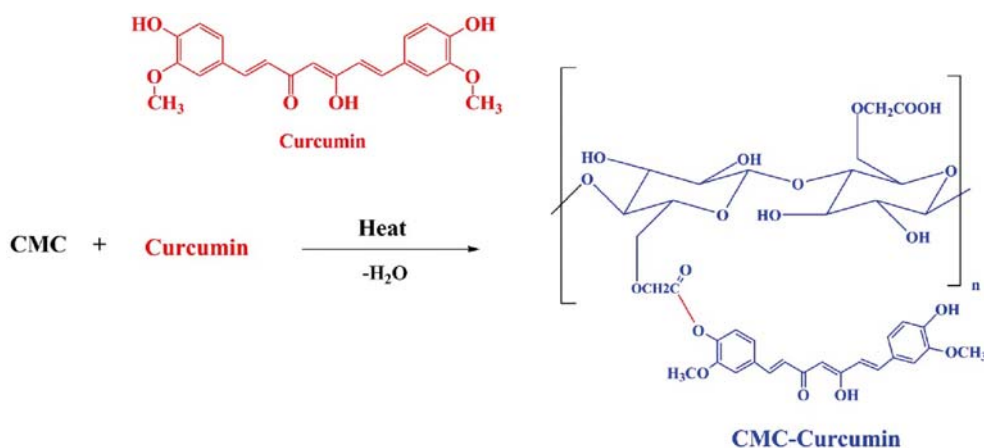
#### Chemistry

The chemical reaction of carboxymethyl cellulose (CMC) with curcumin nanoparticles was explained in the following (**Scheme 1**) to form curcumin nanoparticles loaded with carboxymethyl cellulose as an acarbose analog. The reaction is classified as esterification reaction in which the hydroxyl group in curcumin make a nucleophilic attack to the carbonyl group in in carboxymethyl group in CMC and forms new ester group after dehydration.

#### Curcumin nanoparticles loaded with carboxymethyl cellulose (CMC-nano-CUR) characterization

#### UV/Vis. spectrum

UV/Vis. Optical absorption spectra represent an important tool for the investigation of the electronic transition combined with their optical band gap for a requested sample. **Figure 2** reveals UV/Vis. optical spectral data of curcumin extract which is a diarylheptanoid, belonging to curcuminoids group (natural phenol liable for plant extract yellow color) with a main absorption band



**Scheme 1.** The reaction of carboxymethyl cellulose (CMC) with curcumin nanoparticles

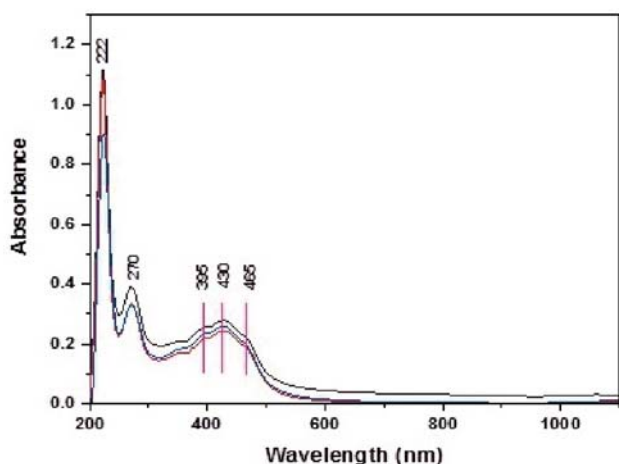


**Figure 2.** UV/Vis. optical absorption spectra of curcumin nanoparticles loaded with carboxymethyl cellulose

centered at 430 nm with two less intense shoulders at about 395 and 465 nm.

The appearance of one or more peaks in the region from 200 to 400 nm is a clear indication of the presence of unsaturated groups and heteroatoms such as S, N, and O atoms<sup>31</sup>.

#### Fourier Transform Infrared Spectroscopy (FT-IR)

The IR spectrum of curcumin showed a noticeable broad stretching band at 3540–3290  $\text{cm}^{-1}$ , attributed to its characteristic two phenolic OH groups (red line in Figure 3). Some other stretching vibrations were also obvious at 1627  $\text{cm}^{-1}$  and 1597  $\text{cm}^{-1}$  due to C=O and C=C, respectively. The FT-IR spectrum of CMC (black line in Figure 3) was used as the standard to confirm the presence of the capping agent on the curcumin sample even after rigorous washing. The band at 3420–3200  $\text{cm}^{-1}$  was attributed to its characteristic OH group, 2922  $\text{cm}^{-1}$  was attributed to the stretching band of aliphatic CH and  $\text{CH}_2$  groups, 1624  $\text{cm}^{-1}$  corresponds to the stretching vibration of carbonyl in the carboxyl group (COO), while the absorption peak at 1432  $\text{cm}^{-1}$  corresponds to the vibration of the sodium carboxylate group. Finally, strong absorption occurs in the wide range of 940–1270  $\text{cm}^{-1}$ , which refers to the fingerprint region<sup>32</sup>. The (CMC-nano-CUR) showed in (the blue line in Figure 3) broad stretching band at 3550–3250  $\text{cm}^{-1}$  related to the hydroxyl group and the 1635  $\text{cm}^{-1}$

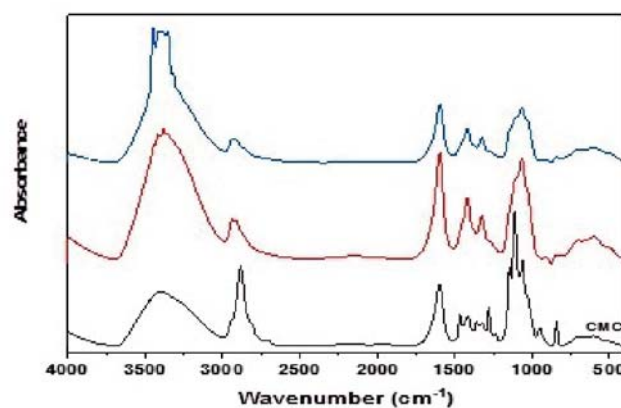


**Figure 3.** FTIR of the prepared curcumin nanoparticles loaded with carboxymethyl cellulose

corresponds to the stretching vibration of carbonyl in the carboxyl ester (COO) newly formed.

#### Transmission electron microscopy (TEM)

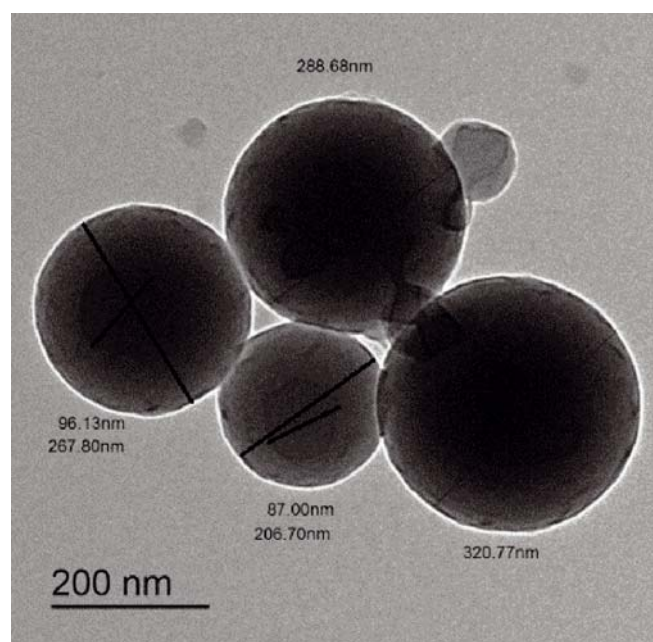
The loading of curcumin nanoparticles onto the CMC has increased the solubility of curcumin in the aqueous media as the CMC is hydrophilic in nature, small in size, and has a large surface area. This allows for greater interaction with the aqueous solvent, thus resulting in an increase in curcumin solubility in aqueous media.

Figure 4 reveals a TEM image of the curcumin-encapsulated polymeric matrix. The micrograph shows nano-scale curcumin encapsulated microsphere with a radius of 87, 97, 209, 288, and 320 nm.

#### Molecular docking validation

$\alpha$ -Amylase (also known as  $\alpha$ -1,4-glucan-4-glucanohydrolase, EC 3.2.1.1) is responsible for catalyzing the hydrolysis of  $\alpha$ -D-(1,4)-glucosidic linkages in substances such as starch, glycogen, and various oligosaccharides, resulting in the release of  $\alpha$ -anomeric products. This particular enzyme has been extensively investigated from several angles, including its structure and function, secretion mechanisms, as well as its application in industrial settings. Researchers have successfully determined the three-dimensional X-ray structures of  $\alpha$ -amylases, specifically those derived from human salivary glands<sup>33</sup>.

These comprehensive studies have provided valuable insights into the overall folding pattern of  $\alpha$ -amylase. The presented Figure 5 discusses the binding interac-



**Figure 4.** TEM image of the curcumin-encapsulated polymeric matrix

tion between the amino acid residues of  $\alpha$ -amylase with different presented ligands like curcumin, CMC, nano synthesized CUR supported CMC, and acarbose as reference drug ligand.

The data obtained show that the targeted synthesized ligand, curcumin nanoparticles loaded with carboxymethyl cellulose (CMC-nano-CUR, see Figure 5B and Figure 7A) forming more than five bonds with the residues of  $\alpha$ -amylase and comparing with the bonding in reference

molecule (Acarbose, Figure 5A) which gives four bonds with the residues of  $\alpha$ -amylase.

The calculated energy score ( $E$ -score) values are a significant factor in evaluating the ligand-enzyme interaction in which the low value of the  $E$ -score (kcal/mol) gives more good interaction. The data summarized in Table 1 explains that the lowest values were obtained when the prepared CUR-CMC binding with  $\alpha$ -amylase. Then, the CUR-supported CMC can be presented as a good analog for the acarbose drug for treating hyperglycemia.

**Table 1.** The  $E$ -score (kcal/mol) for the interaction between  $\alpha$ -amylase enzyme with different ligands CUR, CMC, CUR-CMC, and Acarbose

| Ligands    | CUR         | CMC         | CUR-CMC     | Acarbose    |
|------------|-------------|-------------|-------------|-------------|
| $E$ -score | -5.57478762 | -7.62639666 | -9.97210789 | -8.45353794 |

$\alpha$ -Glucosidase (AGase) is an enzyme that belongs to the category of retaining glycosidases. Its primary function is to hydrolyze the  $\alpha$ -glucosidic linkage at the non-reducing end of substrates. This particular enzyme is an integral part of the amyolytic pathway in a diverse range of organisms, including bacteria, plants, and animals<sup>34-36</sup>. There are three distinct groups into which AGase can be classified based on its substrate specificity. The enzymes belonging to group I exhibit a preference for heterogeneous substrates like sucrose and aryl  $\alpha$ -glucosides, whereas enzymes in groups II and III are specifically tailored to homogeneous substrates. It is important to note that enzymes in group III possess a heightened activity towards long-chain substrates. In addition to its hydrolytic role, AGase also can catalyze trans-glycosylation, which involves the transfer of a glu-

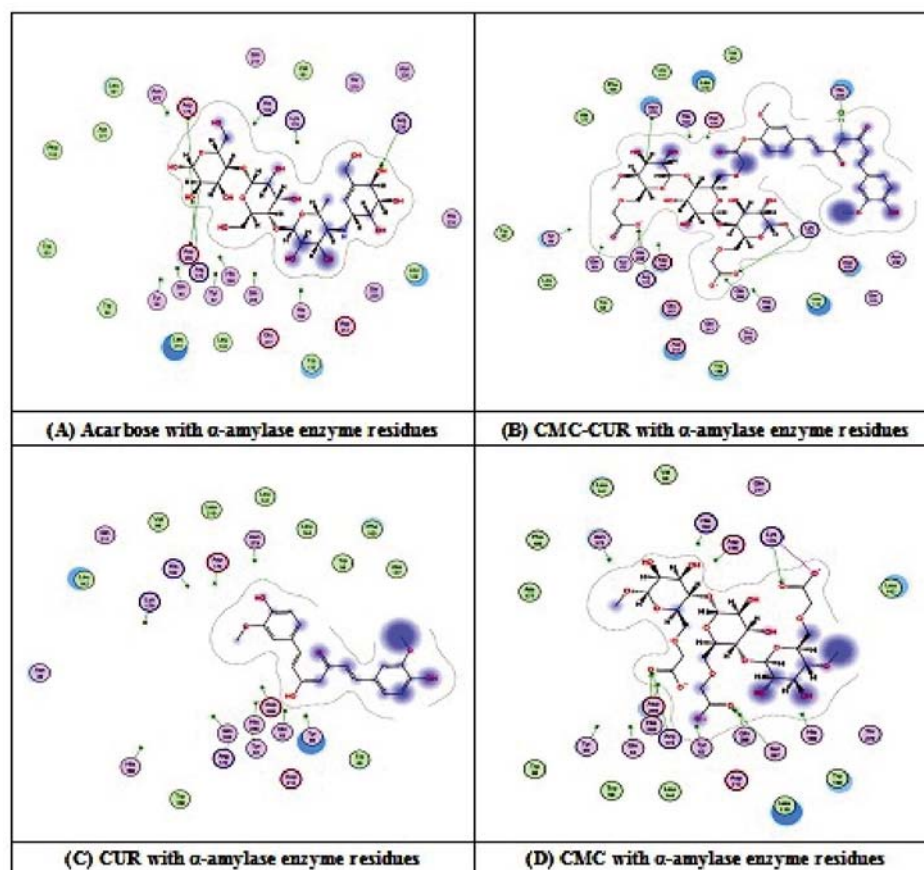


**Figure 5.** (2D) Comparison between Acarbose as a reference molecule, CMC-CUR, CUR, and CMC binding with  $\alpha$ -amylase enzyme residues

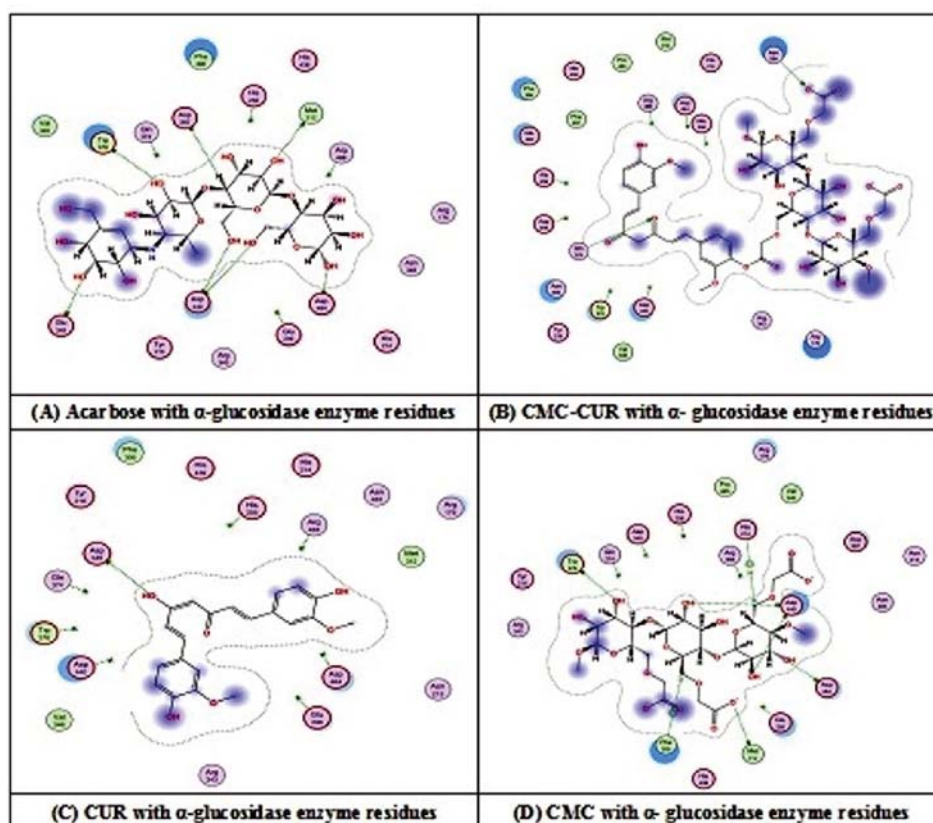


**Figure 6.** (2D) Comparison between Acarbose as a reference molecule, CMC-CUR, CUR, and CMC binding with  $\alpha$ -glucosidase enzyme residues

cosyl residue to an acceptor molecule. This particular activity contributes to the synthesis of oligosaccharides and glucosides<sup>37, 38</sup>.

The presented Figure 6 discusses the binding interaction between the amino acid residues of  $\alpha$ -Glucosidase (AGase) with different presented ligands like curcumin, CMC, nano synthesized CUR supported CMC, and acarbose as reference drug ligand.

The data obtained show that the targeted synthesized ligand (nano CMC-CUR, see Figure 6B and Figure 7B) forms more than five bonds with the residues of  $\alpha$ -amylase

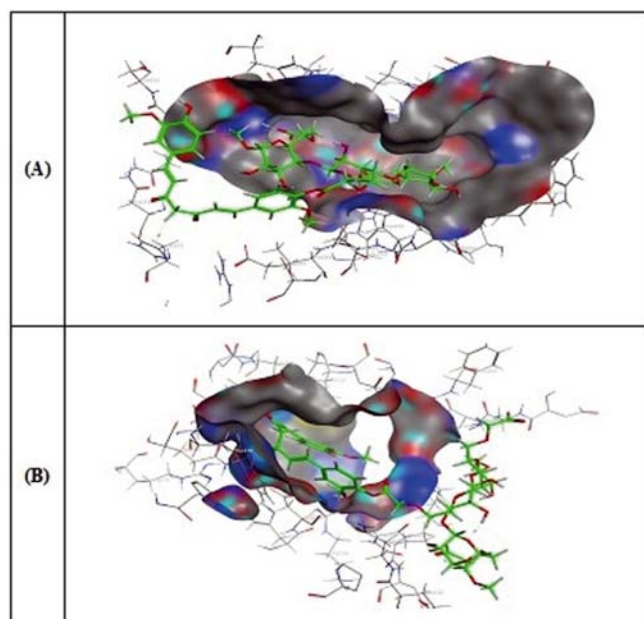


**Figure 7.** (3D) of CMC-CUR with (A)  $\alpha$ -amylase enzyme residues and (B)  $\alpha$ -glucosidase enzyme residues

**Table 2.** The  $E$ -score (kcal/mol) for the interaction between  $\alpha$ -Glucosidase with different ligands CUR, CMC, CUR-CMC, and Acarbose

| Ligands    | CUR         | CMC         | CUR-CMC     | Acarbose    |
|------------|-------------|-------------|-------------|-------------|
| $E$ -score | -5.73889494 | -8.39424038 | -8.07682037 | -8.52121449 |

and comparing with the bonding in reference molecule (Acarbose, Figure 6A) which gives four bonds with the residues of  $\alpha$ -amylase.

The calculated energy score ( $E$ -score) values are a significant factor in evaluating the ligand-enzyme interaction in which the low value of  $E$ -score (kcal/mol) gives more good interaction. The data summarized in Table 2 explains that the lowest values obtained in the case of CMC and CUR-CMC compared with acarbose binding with  $\alpha$ -Glucosidase (AGase). Then, the CUR-supported CMC can be presented as a good analog for the acarbose drug for treating hyperglycemia.

## CONCLUSION

In summary of this work, curcumin nanoparticles were successfully prepared from commercial CUR powder “XPRS Nutra organic turmeric curcumin powder extract 10:1 - premium USDA” using the hydrothermal squeeze method. Curcumin-loaded polymer nanocomposite thin films were prepared *via* a traditional solution casting routine in aqueous media. The target product was confirmed using UV/Vis and FTIR spectroscopy, combined with transmission electron microscopy (TEM). The TEM image shows the spherical shape of curcumin-loaded CMC with a radius ranging from 87 to 320 nm. Molecular docking and energy score value studies of curcumin (CUR), carboxymethyl cellulose (CMC), and curcumin nanoparticles loaded with carboxymethyl cellulose (CUR-

-CMC) were performed as  $\alpha$ -amylase and  $\alpha$ -glucosidase inhibitors for diabetes mellitus treatment.

In the future, the results will motivate us to extend the biological evaluation, *in vitro* and *in vivo* studies, of the curcumin-supported CMC as a diabetes mellitus drug.

## ACKNOWLEDGMENTS

The authors are grateful to King Saud University, Riyadh, Saudi Arabia for funding the work through Researchers Supporting Project No. (RSPD2024R852).

## LITERATURE CITED

- Sugandh, F., Chandio, M., Raveena, F., Kumar, L., Karishma, F., Khuwaja, S., Memon, U.A., Bai, K., Kashif, M., Varrassi, G., Khatri, M. & Kumar, S. (2023). Advances in the Management of Diabetes Mellitus: A Focus on Personalized Medicine. *Cureus* 15(8), e43697. DOI: 10.7759/cureus.43697.
- Rosengren, A. & Dikaoui, P. (2023). Cardiovascular outcomes in type 1 and type 2 diabetes. *Diabetologia* 66, 425–437. DOI: 10.1007/s00125-022-05857-5.
- Joshua, S.R. Shin, S. Lee, J.H. & Kim, S.K. (2023). Health to Eat: A Smart Plate with Food Recognition, Classification, and Weight Measurement for Type-2 Diabetic Mellitus Patients' Nutrition Control. *Sensors* 23(3), 1656. DOI: 10.3390/s23031656.
- Padhi, S. Nayak, A.K. & Behera, A. (2020). Type II diabetes mellitus: a review on recent drug based therapeutics. *Biomed. Pharmacother.* 131, 110708. DOI: 10.1016/j.biopha.2020.110708.
- Kwon, S., Kim, Y.C., Park, J.Y., Lee, J., An, J.N., Kim, C.T., Oh, S., Park, S., Kim, D.K., Oh, Y.K. & Kim, Y.S. (2020). The long-term effects of metformin on patients with type 2 diabetic kidney disease. *Diabetes Care* 43(5), 948–955. DOI: 10.2337/dc19-0936.
- Zahra, S., Zaib, S. & Khan, I. (2024). Identification of isobenzofuranone derivatives as promising antidiabetic agents: Synthesis, *in vitro* and *in vivo* inhibition of  $\alpha$ -glucosidase and  $\alpha$ -amylase, computational docking analysis and molecular dynamics simulations. *Int. J. Biol. Macromol.* 259(part 2), 129241. DOI: 10.1016/j.ijbiomac.2024.129241.
- Lam, T.P., Tran, N.V.N., Pham, L.H.D., Lai, N.V.T., Dang, B.T.N., Truong, N.L.N., Nguyen-Vo, S.K., Hoang, T.L., Mai, T.T. & Tran, T.D. (2024). Flavonoids as dual-target inhibitors against  $\alpha$ -glucosidase and  $\alpha$ -amylase: a systematic review of *in vitro* studies. *Nat. Prod. Bioprospect.* 14, 4. DOI: 10.1007/s13659-023-00424-w.
- Bhawana, Basniwal, R.K., Buttar, H.S., Jain, V.K. & Jain, N. (2011). Curcumin nanoparticles: preparation, characterization, and antimicrobial study. *J. Agric. Food Chem.* 59(5), 2056–2061. DOI: 10.1021/jf104402t.
- Slika, L. & Patra, D. (2020). A short review on chemical properties, stability and nano-technological advances for curcumin delivery. *Expert Opin. Drug Deliv.* 17(1), 61–75. DOI: 10.1080/17425247.2020.1702644.
- Ataei, M., Garekani, H.A., Sani, M.A., McClements, D.J. & Sadeghi, F. (2024). Evaluation of polyvinyl pyrrolidone nanofibers for encapsulation, protection, and release of curcumin: Impact on *in vitro* bioavailability. *J. Mol. Liq.* 397, 124115. DOI: 10.1016/j.molliq.2024.124115.
- Islam, M.R., Rauf, A., Akash, S., Trisha, S.I., Nasim, A.H., Akter, M., Dhar, P.S., Ogaly, H.A., Hemeg, H.A., Wilairatana, P. & Thiruvengadam, M. (2024). Targeted therapies of curcumin focus on its therapeutic benefits in cancers and human health: Molecular signaling pathway-based approaches and future perspectives. *Biomed. Pharmacother.* 170, 116034. DOI: 10.1016/j.biopha.2023.116034.
- Varshney, H. & Siddique, Y.H. (2024). Effect of Natural Plant Products on Alzheimer's Disease. *CNS Neurol. Disord.*

*Drug Targets* 23(2), 246–261. DOI: 10.2174/1871527322666230228102223.

- Rahman, M.S., Hasan, M.S., Nitai, A.S., Nam, S., Karmakar, A.K., Ahsan, M.S., Shiddiky, M.J.A. & Ahmed, M.B. (2021). Recent Developments of Carboxymethyl Cellulose. *Polymers* 13(8), 1345. DOI: 10.3390/polym13081345.
- Zennifer, A., Senthilvelan, P., Sethuraman, S. & Sundaramurthi, D. (2021). Key advances of carboxymethyl cellulose in tissue engineering & 3D bioprinting applications. *Carbohydr. Polym.* 256, 117561. DOI: 10.1016/j.carbpol.2020.117561.
- Yaradoddi, J.S., Banapurmath, N.R., Ganachari, S.V., Soudagar, M.E.M., Mubarak, N.M., Hallad, S., Hugar, S. & Fayaz, H. (2020). Biodegradable carboxymethyl cellulose based material for sustainable packaging application. *Sci. Rep.* 10, 21960. DOI: 10.1038/s41598-020-78912-z.
- Zhang, W., Liu, Y., Xuan, Y. & Zhang, S. (2020). Synthesis and Applications of Carboxymethyl Cellulose Hydrogels. *Gels* 8(9), 529. DOI: 10.3390/gels8090529.
- Muhammed, M.T. & Aki-Yalcin, E. (2024). Molecular docking: principles, advances, and its applications in drug discovery. *Lett. Drug Des. Discov.* 21(3), 480–495. DOI: 10.2174/1570180819666220922103109.
- Kolybalov, D.S., Kadtsyn, E.D. & Arkhipov, S.G. (2024). Computer Aided Structure-Based Drug Design of Novel SARS-CoV-2 Main Protease Inhibitors: Molecular Docking and Molecular Dynamics Study. *Computation* 12(1), 18. DOI: 10.3390/computation12010018.
- Zerroug, E., Belaidi, S., Chtita, S., Tuffaha, G., AbulQais, F., Kciuk, M., Dubey, A. & Taha, M.O. (2024). Structure-Based Approaches for the Prediction of Alzheimer's Disease Inhibitors: Comparative Interactions Analysis, Pharmacophore Modeling and Molecular Dynamics Simulations. *Chem. Select* 9(6), e202303307. DOI: 10.1002/slct.202303307.
- Hassan, A.S., Osman, S.A. & Hafez, T.S. (2015). 5-Phenyl-2-furaldehyde: Synthesis, reactions and biological activities. *Egypt. J. Chem.* 58(2), 113–139. DOI: 10.21608/ejchem.2015.978.
- Morsy, N.M., Hassan, A.S., Hafez, T.S., Mahran, M.R.H., Sadawe, I.A. & Gbaj, A.M. (2021). Synthesis, antitumor activity, enzyme assay, DNA binding and molecular docking of Bis-Schiff bases of pyrazoles. *J. Iran. Chem. Soc.* 18(1), 47–59. DOI: 10.1007/s13738-020-02004-y.
- Alkahtani, H.M., Almehizia, A.A., Al-Omar, M.A., Obaidullah, A.J., Zen, A.A., Hassan, A.S., & Aboulthana, W.M. (2023). *In vitro* evaluation and bioinformatics analysis of Schiff bases bearing pyrazole scaffold as bioactive agents: antioxidant, anti-diabetic, anti-Alzheimer, and anti-arthritis. *Molecules* 28(20), 7125. DOI: 10.3390/molecules28207125.
- Hassan, A.S., Morsy, N.M., Aboulthana, W.M. & Ragab, A., 2023. *In vitro* enzymatic evaluation of some pyrazolo-[1,5-*a*]pyrimidine derivatives: Design, synthesis, antioxidant, anti-diabetic, anti-Alzheimer, and anti-arthritis activities with molecular modeling simulation. *Drug Dev. Res.* 84(1), 3–24. DOI: 10.1002/ddr.22008.
- Naglah, A.M., Askar, A.A., Hassan, A.S., Khatab, T.K., Al-Omar, M.A., & Bhat, M.A. (2020). Biological Evaluation and Molecular Docking with In Silico Physicochemical, Pharmacokinetic and Toxicity Prediction of Pyrazolo[1,5-*a*]pyrimidines. *Molecules* 25(6), 1431. DOI: 10.3390/molecules25061431.
- Khatab, T.K., Mubarak, A.Y., & Soliman, H.A. (2017). Design and synthesis pairing between xanthene and tetrazole in pentacyclic system using tetrachlorosilane with aurora kinase inhibitor validation. *J. Heterocycl. Chem.* 54(4), 2463–2470. DOI: 10.1002/jhet.2846.
- Khatab, T.K., Hassan, A.S. & Hafez, T.S. (2019). V2O5/SiO2 as an efficient catalyst in the synthesis of 5-amino-pyrazole derivatives under solvent free condition. *Bull. Chem. Soc. Ethiop.* 33(1), 135–142. DOI: 10.4314/bcse.v33i1.13.
- Shin, Y., Blackwood, J.M., Bae, I.T., Arey, B.W. & Exarhos, G.J. (2007). Synthesis and stabilization of selenium

nanoparticles on cellulose nanocrystal. *Mater. Lett.* 61(21), 4297–4300. DOI: 10.1016/j.matlet.2007.01.091.

28. Shaker, N., Kandil, E.M., Osama, Y., & Khatab, T.K. (2021). ZnCl<sub>2</sub>/SiO<sub>2</sub> as a New Catalyst for the Eco-Friendly Synthesis of N-Thiocarbamoyl Pyrazoles and Thiosemicarbazones with Antioxidant and Molecular Docking Evaluation as (Upps) Inhibitor. *Curr. Org. Chem.* 25(17), 2037–2044. DOI: 10.2174/1385272825666210809142341.

29. Hassan, A.S., Morsy, N.M., Aboulthana, W.M. & Ragab, A. (2023). Exploring novel derivatives of isatin-based Schiff bases as multi-target agents: design, synthesis, *in vitro* biological evaluation, and *in silico* ADMET analysis with molecular modeling simulations. *RSC Adv.* 13(14), 9281–9303. DOI: 10.1039/D3RA00297G.

30. Khatab, T.K., Kandil, E.M., Elsefy, D.E. & El-Mekabaty, A. (2021). A one-pot multicomponent catalytic synthesis of new 1*H*-Pyrazole-1-Carbothioamide derivatives with molecular docking studies as COX-2 inhibitors. *Biointerface Res. Appl. Chem.* 11(6), 13779–13789. DOI: 10.33263/BRIAC116.1377913789.

31. Klages, C.P., Hinze, A. & Khosravi, Z. (2013). Nitrogen plasma modification and chemical derivatization of polyethylene surfaces-an in situ study using FTIR-ATR spectroscopy. *Plasma Process. Polym.* 10(11), 948–958. DOI: 10.1002/ppap.201300033.

32. Hidayat, S., Ardiaksa, P., Riveli, N. & Rahayu, I. (2016). Synthesis and characterization of carboxymethyl cellulose (CMC) from salak-fruit seeds as anode binder for lithium-ion battery. *J. Phys.: Conf. Ser.* 1080, 012–017. DOI: 10.1088/1742-6596/1080/1/012017.

33. Fujimoto, Z., Takase, K., Doui, N., Momma M., Matsumoto, T. & Mizuno, H. (1998). Crystal structure of a catalytic-site mutant alpha-amylase from *Bacillus subtilis* complexed with maltopentaose. *J. Mol. Biol.* 277(2), 393–407. DOI: 10.1006/jmbi.1997.1599.

34. Konishi, Y., Okamoto, A., Takahashi, J., Aitani, M. & Nakatani, N. (1994). Effect of Bay m 1099, an  $\alpha$ -glucosidase inhibitor, on starch metabolism in germinating wheat seeds. *Biosci. Biotechnol. Biochem.* 58(1), 135–139. DOI: 10.1271/bbb.58.135.

35. Kimura, A. (2000). Molecular anatomy of  $\alpha$ -glucosidase. *Trends Glycosci. Glycotechnol.* 12, 373–380. DOI: 10.4052/tigg.12.373.

36. Okuyama, M., Saburi, W., Mori, H. & Kimura, A. (2016).  $\alpha$ -Glucosidases and  $\alpha$ -1, 4-glucan lyases: structures, functions, and physiological actions. *Cell. Mol. Life Sci.* 73, 2727–2751. DOI: 10.1007/s00018-016-2247-5.

37. Yamamoto, T., Unno, T., Sugawara, M. & Goda, T. (1999). Properties of a nigerose and nigerosylmaltooligosaccharides-supplemented syrup. *J. Appl. Glycosci.* 46(4), 475–482. DOI: 10.5458/jag.46.475.

38. Ojima, T., Aizawa, K., Saburi, W. & Yamamoto, T. (2012).  $\alpha$ -Glucosylated 6-gingerol: chemoenzymatic synthesis using  $\alpha$ -glucosidase from *Halomonas* sp. H11, and its physical properties. *Carbohydr. Res.* 354, 59–64. DOI: 10.1016/j.carres.2012.03.012.